Available online at www.sciencedirect.com
ScienceDirect
Polymer 48 (2007) 4152–4165
polymer
www.elsevier.com/locate/polymer

Shear thickening behavior of dilute poly(diallyl dimethyl ammonium chloride) aqueous solutions

Wen-Hong Liu, T. Leon Yu*, Hsiu-Li Lin

Department of Chemical Engineering and Materials Science, Yuan Ze University, Nei-Li, Chung-Li, Taoyuan 32003, Taiwan

Received 4 September 2006; received in revised form 24 April 2007; accepted 2 May 2007
Available online 13 May 2007

Abstract

Using dynamic light scattering (DLS) and capillary dynamic viscoelasticity (DVE) analyzer, we investigated dilute (0.5 mg/ml) poly(diallyl dimethyl ammonium chloride) (PDADMAC) aqueous solution properties for three different molecular weights of PDADMACs mixed with various concentrations of NaCl. The dependence of PDADMAC molecular chain conformations in aqueous solutions on polymer molecular weight and NaCl concentration were studied. By analyzing dynamic shear viscosity $\eta'(\omega)$, viscoelastic relaxation times t_r, and shear rate at tube wall $\acute{r}_a(\omega)$ of PDADMAC aqueous solutions in oscillatory flows, we proposed that polymer chain conformations varied with increasing shear frequency ω via the following steps: intra-polymer associations, dissociation of intra-polymer associations, stretching of polymer chains, inter-polymer aggregations, and dissociations of inter-polymer aggregations. The intra-polymer associations lowered the n' exponent of storage modulus $G'(\omega)$ ($G'(\omega) \sim \omega^{n'}$) with $n' < 2$, and the polymer chain stretching and inter-polymer aggregations caused shear thickening (i.e. upturn of $\eta'(\omega)$) of PDADMAC aqueous solutions. The behaviors of the lowering of n' exponent with $n' < 2$ and the shear thickening were favored by increasing ionic strength of solutions. By comparing $\eta'(\omega)$ data with DLS hydrodynamic radii (R_h) data, we also confirmed the possibility of inter-polymer aggregations in dilute solutions when polymer chains were stretched in oscillatory flows.

Keywords: Poly(diallyl dimethyl ammonium chloride); Dilute solutions; Shear thickening

1. Introduction

Most of the polymer solutions display shear thinning behavior. Shear thickening, however, is not so frequently observed as shear thinning, and has been observed in polystyrene solutions in decalin [1,2], polystyrene solutions in toluene [3], crystallizable polymer solutions such as polyethylene in xylene and polypropylene in tetralin [4], polyethyleneoxide in ethanol and water [4,5], aqueous solutions with polymers consisting of charged and hydrophobic compositions [6,7], aqueous solutions with mixtures of water-soluble polymers and colloidal particles [8], worm-like micelles solutions, and ionomers solutions etc [9–11]. Under flow at low shear rates these solutions exhibit shear thinning or Newtonian behavior; shear thickening occurs when shear rate is increased above a critical shear rate. However, when shear rate is further increased, shear thinning behavior is observed.

Most of the researchers investigated shear thickening behavior of polymer solutions near the overlap concentration. The mechanism for shear thickening is still a matter of discussion. Various explanations have been proposed to account for the shear thickening behavior of polymer solutions. One of the most accepted explanations is the ''flow-induced formation of macromolecular associations'' [1,4,12–14], which had been confirmed by Kishbaugh and McHugh using in situ simultaneous optical and rheological observations of polymer solutions in a coquette flow cell [1]. To explain the shear thickening behavior of associative polymer solutions near overlap concentration, several theoretical approaches and simulation models [14–23] had appeared in the past two decades. Witten and Cohen [15] proposed a shear thickening mechanism in the framework of mean field approximation. They showed that

* Corresponding author. Tel.: +886 3 4638800x2553; fax: +886 3 4559373.
E-mail address: cetlyu@saturn.yzu.edu.tw (T.L. Yu).

0032-3861/$ - see front matter © 2007 Elsevier Ltd. All rights reserved.
doi:10.1016/j.polymer.2007.05.012

shear flow can increase the probability of inter-chain association at the expense of intra-chain association, thus leading to the increase of viscosity. This mechanism was based on an increasing number of inter-molecular associations due to the stretching of the polymer chains under flow. Ballard et al. [16] also predicted that shear thickening occurs in a flow field of sufficiently high strain rate due to the expansion of self-associating polymers. Wang [19] attributed shear thickening to the coagulation of free chains into existing transient network and thus there is an enhancement of the effective network molecular chains and viscosity. Ma and Cooper [20] related shear thickening to extended non-Gaussian chains induced by shear and the partial relaxation of dissociated extended chains. They claimed the possibility of the recapture of dissociated extended chains by the associating networks before the dissociated chains fully relaxed to an equilibrium state causing an enhancement of thickening behavior.

In literature, most of papers reported shear thickening behavior of polymer solutions near overlap concentrations. Few papers reported shear thickening behavior of dilute polyelectrolyte solutions with various ionic strengths. In the present study, using capillary dynamic viscoelasticity (DVE) analyzer, static light scattering (SLS), and dynamic light scattering (DLS), we investigated dilute aqueous solution properties of three different molecular weights of poly(diallyl dimethyl ammonium chloride) (PDADMAC) mixed with various concentrations of NaCl. The dependence of polymer chain conformations and dynamic viscoelastic properties of these polymer solutions on PDADMAC molecular weight and NaCl concentration were studied. The dynamic shear viscosity data showed shear thickening behavior with increasing shear frequency, when the polyion solution was in an oscillatory flow in a capillary rheometer. The storage modulus data showed deviation of n' exponent ($G'(\omega) \sim \omega^{n'}$) from that of Rouse and Zimm model of ordinary dilute polymer solutions. By comparing shear viscosity data with DLS hydrodynamic radius data, we suggested that shear thickening of dilute polyion solutions was attributed to the polymer chain stretching and inter-polymer aggregations. The behavior of shear thickening was favored by increasing ionic strength of solutions, which can be attributed to the reduction of inter-polymer electrostatic charge repulsion caused by the electrostatic shielding of the charged groups of polyions by excess salt.

PDADMAC is a cationic water soluble polymer. It was synthesized from diallyl dimethyl ammonium chloride (DADMAC) via free radical polymerization. The polymerization kinetics and mechanism, chemical structure, and molecular weight distribution measurements had been well studied and reported in literature [24–30].

The oscillating capillary rheometer was a Vilastic VE system rheometer. The advantage of Vilastic VE rheometer is its capability to obtain precise dynamic viscoelastic data of dilute polymer solutions with small sample sizes ($\sim$3 ml) and solution viscosities lower than 0.2 poise. In this rheometer, a chamber containing silicone oil with an oscillatory flow generator, is installed at the bottom of a sample solution reservoir. The measuring capillary tube is inserted vertically in the center of the sample solution reservoir and filled with sample solution. The fluid inside the tube for the dynamic viscoelasticity measurements is separated from the silicon oil by a Teflon membrane. The fluid in the measuring tube was forced into oscillatory flow from silicone oil by an electrodynamic transducer with a constant drive. The pressure gradient P along and volume flow U through the tube were monitored by sensors at the entrance of the tube. The instrument provides resolutions of ''magnitude'' and ''phase'' of P. The ''magnitude'' and ''phase'' of P combining with U allows calculation of the viscous and elastic components of shear stress, and also the shear rate at the tube wall. The DVE data such as dynamic shear viscosity (DSV) $\eta'(\omega)$, shear elasticity $\eta''(\omega)$, storage shear modulus $G'(\omega)$, and loss shear modulus $G''(\omega)$ etc were derived from viscouse component and elastic component of shear stress and shear rate. The detailed instrument design and theory can be found in Refs. [31–33].

2. Experimental section

2.1. Material and sample preparations

2.1.1. Poly(diallyl dimethyl ammonium chloride) (PDADMAC)

Three PDADMACs (Aldrich Chemical Co), i.e. PDADMAC-1 ($M_w = 1.5 \times 10^5$ g/mol), PDADMAC-2 ($M_w = 3.2 \times 10^5$ g/mol), and PDADMAC-3 ($M_w = 4.5 \times 10^5$ g/mol) were used in this study. The indicated M_ws were obtained from Aldrich Chemical Co.

2.1.2. Sodium chloride

Sodium chloride (Riedel de Haen Co., Germany) was used as calibrated NaCl aqueous solutions in differential refractive index increment dn/dC measurements and a salt of PDADMAC aqueous solution.

2.1.3. Sample preparations

The aqueous solutions of three PDADMACs with PDADMAC concentrations of 0.5, 1.0, 1.5, 2.0, and 2.5 mg/ml and a NaCl concentration of 1.0 M were prepared from deionized water. These solutions after dialysis with a Spectra Pore membrane (MWCO = 3000) and filtered through a 0.45 μm Millipore filter were used for refractive index increment dn/dC and SLS measurements. The 0.5 mg/ml PDADMAC aqueous solutions mixed with NaCl concentrations ranging from 0.0 to 1.0 M were prepared and used for DLS and DVE measurements. Before DLS measurements, the PDADMAC aqueous solutions were filtered through a 0.45 μm Millipore filter. All the measurements were carried out at 25 + 0.5 °C.

2.2. Instrumentation

2.2.1. Refractometer

Abe refractometer (Nippon Optical Works, Tokyo) was used for the measurements of refractive indices of NaCl aqueous solutions.

2.2.2. Differential refractometer

A RF600 differential refractometer (C.N. Wood, PA) was used to determine differential refractive index increments dn/dC of polymer solutions. The measurements were calibrated using NaCl aqueous solutions [34].

2.2.3. Static light scattering

A BI-200SM goniometer with a photo detector designed in a BI2030AT correlator (Brookhaven Co, NY) and an Ar ion laser (514 nm, Lyconix, operated at 100 mW) were used for SLS measurements. Second virial coefficients A_2, radii of gyration R_G, and molecular weights M_w of PDADMAC aqueous solutions were obtained from these measurements.

2.2.4. Dynamic light scattering

The dynamic light scattering measurements were carried out using a 256-channel autocorrelator (model BI9000, Brookhaven Co., NY) and an Ar ion laser (514 nm, Lyconix, operated at 100 mW). The measurements were performed at various scattering angles $\theta = 30°, 45°, 60°, 90°$, and 120°. To obtain the hydrodynamic radius (R_h) distributions of PDADMAC, an inverse Laplace transformation (ILT) was made from the normalized field autocorrelation function $g^{(1)}(t)$ by using CONTIN software and Stokes–Einstein equation.

2.2.5. Dynamic viscoelasticity analyzer

An oscillatory flow rheometer (VE system, Vilastic Scientific Inc., Texas) with a cylindrical tube of length 6.115 cm and inner diameter 0.0513 cm was used for DVE measurements.

3. Results and discussion

3.1. SLS measurements

The scattered light intensity from a polymer solution is given by [35,36]

$$KC/\Delta R_\theta = (1/M_w)\left[1 + \left(16\pi^2\langle R_G^2\rangle/3\lambda^2\right)\sin^2(\theta/2) + \ldots\right] + 2A_2C + \ldots \quad (1)$$

where ΔR_θ is the excess Rayleigh ratio of a polymer solution at a scattering angle θ, λ the wavelength of incident light, A_2 the second virial coefficient, $\langle R_G^2\rangle$ the mean square radius of gyration of polymers in a solution, and C the polymer concentration. For vertically polarized incident light, the optical constant, K, is given by

$$K = 4\pi^2 n_o^2 (dn/dC)^2/\left(\lambda^4 N_A\right) \quad (2)$$

where n_o is the refractive index of the solvent, N_A the Avogadro's number, and dn/dC the differential refractive increment of a polymer solution. Zimm plots were constructed and extrapolated to zero concentration and zero scattering angle using Eq. (1). The refractive index n_o of 1.0 M NaCl aqueous solution was measured using an Abe refractometer and a value of 1.354 was obtained. The dn/dC values of PDADMAC-1, PDADMAC-2, and PDADMAC-3 aqueous solutions mixed with 1.0 M NaCl measured at 25 °C were 0.1745, 0.1720 and 0.1701 ml/g, respectively.

The Zimm plot of PDADMAC-1 aqueous solutions mixed with 1.0 M NaCl obtained at 25 °C is shown in Fig. 1. The linear extrapolations of $KC/\Delta R_\theta$ to $C \to 0$ and $\theta \to 0$ are also shown in Fig. 1. Similar Zimm plots of other PDADMACs in 1.0 M NaCl aqueous solutions were also obtained and are not shown in the present paper. The M_w, A_2, and $\langle R_G\rangle$ of PDADMAC in 1.0 M NaCl aqueous solutions were obtained from the intercepts and slopes of the extrapolated data (i.e. $C \to 0$ and $\theta \to 0$), respectively, of Zimm plots, and are listed in Table 1. The M_w data obtained in our measurements were quite consistent with those reported from the supplier (Aldrich Chemical Co).

3.2. DLS measurements

The DLS measurements of 0.5 mg/ml PDADMAC aqueous solutions mixed with various concentrations of NaCl were carried out at 25 °C with scattering angles varying from $\theta = 30°$ to $\theta = 120°$. The normalized field autocorrelation functions $g^{(1)}(t)$ and the relaxation times τ distributions $A(\tau)$ at the scattering angle $\theta = 90°$ for 0.5 mg/ml PDADMAC-3 aqueous solutions mixed with 0.0–1.0 M NaCl are shown in Fig. 2. Fig. 3 shows plots of average relaxation rate $\langle 1/\tau\rangle$ versus $\sin^2\theta/2$ for 0.5 mg/ml PDADMAC-3 aqueous solutions mixed with various concentrations of NaCl. The linear plots of $\langle 1/\tau\rangle$ against $\sin^2\theta/2$ suggest diffusive relaxation modes of these data. Similar diffusive behavior was also obtained for other PDADMAC aqueous solutions.

On careful investigation of Fig. 2, we found a fast relaxation mode located at $\log t < 0.5$ μs while [NaCl] ≥ 0.07 M.

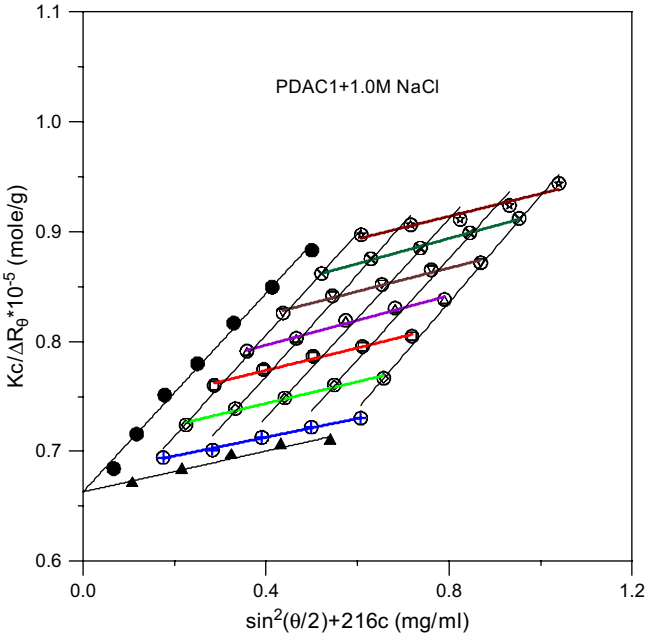

Fig. 1. Zimm plot of PDADMAC-1 in 1.0 M NaCl aqueous solution: (○) experimental data of $KC/\Delta R_\theta$; (▲) data of $KC/\Delta R_\theta$ linear extrapolation to $C \to 0$; (●) data of $KC/\Delta R_\theta$ linear extrapolation to $\theta \to 0$.

Table 1
SLS data of PDADMAC in 1.0 M NaCl aqueous solution

Solution	$M_w \times 10^{-5}$ (g/mol)	$A_2 \times 10^5$ (cm^3 mol/g^2)	$\langle R_G \rangle$ (nm)	$\langle R_G \rangle / \langle R_h \rangle$
PDADMAC-1	1.51	6.71	35.5	1.69
PDADMAC-2	2.35	5.31	45.4	1.68
PDADMAC-3	4.46	4.81	61.4	1.69

The DLS fast relaxation mode of polyion solutions had been reported in literature and was attributed to the coupled diffusion of polyions and counterions [28,37–39]. Since the present $g^1(t)$ did not reach an asymptote as $\log t \to 0$ and our main purpose of the present study was to investigate the relation of particles size to shear viscosities of polymer solutions, only slow relaxation modes were analyzed and hydrodynamic radii distribution calculations were performed. The DLS slow mode (1.5 μs < log t < 3.0 μs in this study) of polyion solutions with low ionic strength was also an interesting research topic in the past two decades [37,40–43]. Most of the researchers attributed slow diffusion modes to the internal motion of large domains consisting of a large number of polyions, with slow mode diffusion coefficient D_s increasing linearly with $\sin^2(\theta/2)$. Xia et al. [39] also reported linear increment of D_s with increasing $\sin^2(\theta/2)$ for 3.0 g/L PDADMAC ($M_w = 10^5$–10^6 g/mol) aqueous solutions without

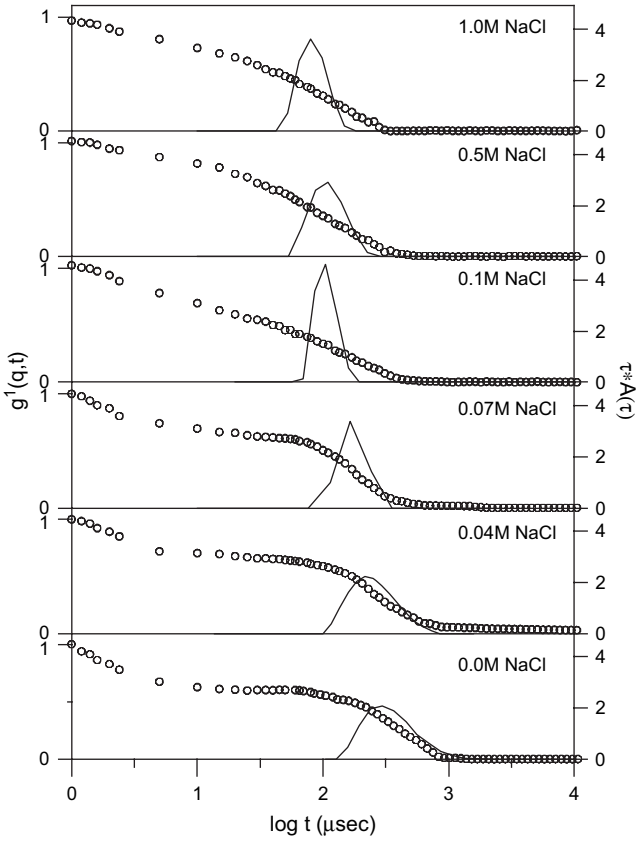

Fig. 2. Normalized field autocorrelation functions $g^{(1)}(t)$ and relaxation time distributions $\tau A(\tau)$ at the scattering angle $\theta = 90°$ for 0.5 mg/ml PDADMAC-3 aqueous solutions mixed with 0.0, 0.04, 0.07, 0.1, 0.5, and 1.0 M NaCl (from bottom to top).

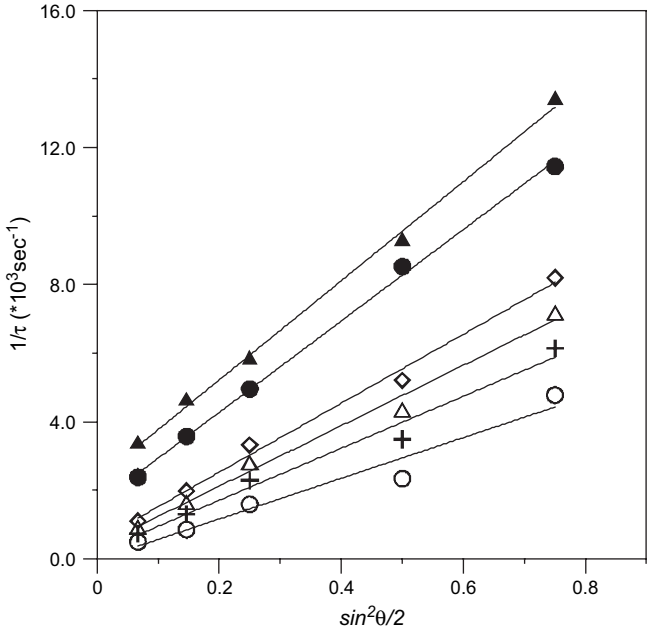

Fig. 3. Plots of relaxation rate $1/\tau$ versus $\sin^2\theta/2$ (scattering angles $\theta = 30°$, 45°, 60°, 90°, and 120°) for 0.5 mg/ml PDADMAC-3 aqueous solutions mixed with various concentrations of NaCl. Concentration of NaCl: (○) 0.0 M; (+) 0.04 M; (△) 0.07 M; (◇) 0.1 M; (●) 0.5 M; (▲) 1.0 M.

mixing salt, indicating internal motions of slow modes. In the present study, the DLS slow relaxation times τ_s were around $10^{1.5}$–$10^{2.7}$ μs (Fig. 2), which were about 10^1 order shorter than those reported by Xia et al. ($\tau_s \sim 10^{3.5}$ μs as shown in Fig. 1 of Ref. [39]). These results indicated that the slow mode particle sizes of our present work were much smaller than those reported by Xia et al. [39]. Thus the present work showed diffusive relaxations of slow modes (Fig. 3). The hydrodynamic radii R_h distributions calculated from Fig. 2 using Stokes–Einstein equation for 0.5 mg/ml PDADMAC-3 aqueous solutions mixed with various concentrations of NaCl are shown in Fig. 4. In calculating R_h distributions from $A(\tau)$, the viscosities of 8.900, 8.906, 8.912, 8.917, 9.109, and 9.353×10^{-3} g cm^{-1} s^{-1} (which were obtained from the measurements using an Ubbelohde viscometer) for 0.00, 0.04, 0.07, 0.10, 0.50, and 1.00 M NaCl aqueous solutions, respectively, were used as viscosities of solvents in Stokes–Einstein equation. These data showed that PDADMAC-3 molecules had largest R_h in an aqueous solution without mixing NaCl. R_h decreased with increasing NaCl concentration in the solutions. Table 2 summarizes $\langle R_h \rangle$ values for PDADMAC aqueous solutions mixed with various concentrations of NaCl. The data of Table 2 show that $\langle R_h \rangle$ decreases with increasing NaCl concentration, indicating the reduction of intra-polymer electrostatic charge repulsion caused by the electrostatic shielding of $\rangle N^+(CH_3)_2$ groups of PDADMACs by the excess Cl^- ions.

From $\langle R_G \rangle$ (Table 1) and $\langle R_h \rangle$ (Table 2) data of PDADMAC in 1.0 M NaCl aqueous solutions, we calculated $\langle R_G \rangle / \langle R_h \rangle$ ratios and values of 1.69, 1.68, and 1.69 were obtained for PDADMAC-1, PDADMAC-2, and PDADMAC-3, respectively (Table 1). During translational motion of particles, the

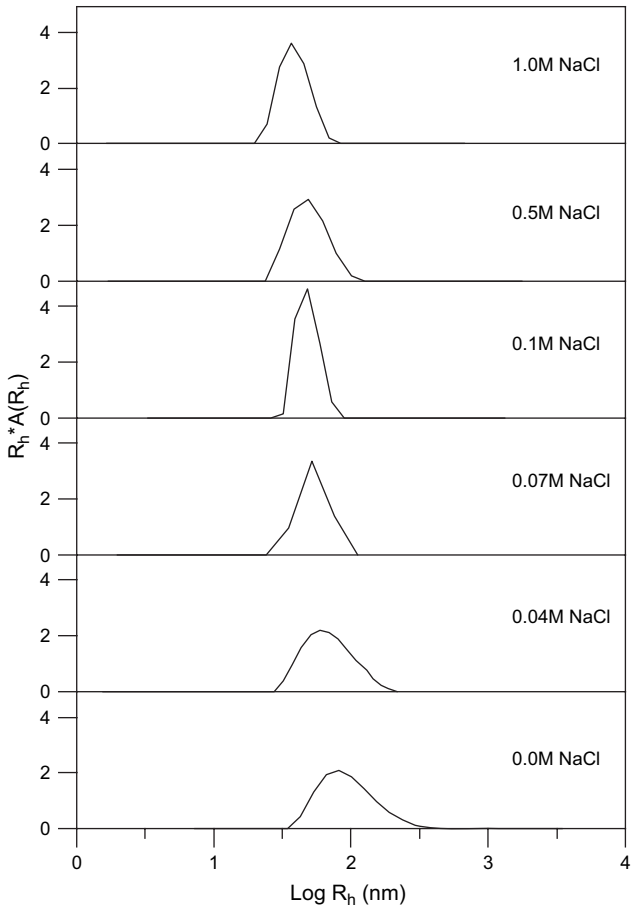

Fig. 4. Hydrodynamic radii R_h distributions calculated from Fig. 2 (scattering angle $\theta = 90°$) using Stokes–Einstein equation for 0.5 mg/ml PDADMAC-3 aqueous solutions mixed with 0.0, 0.04, 0.07, 0.1, 0.5, and 1.0 M NaCl (from bottom to top).

solvent can penetrate deeply into the fairly open molecular chains leading R_h to be smaller than R_G (see Fig. 13.9 of Ref. [44]). However, if the particle is highly compact then only the outer shell is drained by solvent. Thus R_h is larger than R_G for compact molecules (see Fig. 13.9 of Ref. [44]). The ratio $\langle R_G\rangle/\langle R_h\rangle$ is an indicator of the compactness of polymers in solvents. The relation of polymer architecture with $\langle R_G\rangle/\langle R_h\rangle$ ratio in solvents had been summarized by Burchard [44]. According to Burchard, $\langle R_G\rangle/\langle R_h\rangle \geq 2.0$ for rod structural polymers and $\langle R_G\rangle/\langle R_h\rangle = 1.78-1.50$ for polydispersed random coiled polymers. The $\langle R_G\rangle/\langle R_h\rangle = 1.68-1.69$ of present work suggested PDADMAC molecules behaved coil-like structures in 1.0 M NaCl aqueous solutions. On careful investigation of $\langle R_h\rangle$ values shown in Table 2, we found that at a fixed PDADMAC molecular weight, $\langle R_h\rangle$ decreased with increasing NaCl concentration. However, at a fixed NaCl concentration, $\langle R_h\rangle$ increased with increasing PDADMAC molecular weight.

Table 2
DLS $\langle R_h\rangle$ data of PDADMAC aqueous solutions mixed with various concentrations of NaCl

	[NaCl]					
	0.0 M	0.04 M	0.07 M	0.1 M	0.5 M	1.0 M
$\langle R_h\rangle$ (nm)						
PDADMAC-1	44.76	34.02	30.84	27.01	26.10	20.98
PDADMAC-2	61.80	41.88	39.29	35.67	29.35	27.07
PDADMAC-3	81.25	59.06	51.42	48.16	44.78	36.25

3.3. DVE measurements

3.3.1. Dynamic shear viscosity

DVE measurements of 0.5 mg/ml PDADMACs aqueous solutions mixed with 0.0–1.0 M NaCl were carried out at 25 °C. Fig. 5 shows the plots of DSV log $\eta'(\omega)$ versus frequency log ω (ω in unit of rad/s) for PDADMAC-3 aqueous solutions mixed with various concentrations of NaCl. The $\eta'(\omega)$ data show the shear thickening behavior for all of these solutions. The plots of Fig. 5 reveal that PDADMAC aqueous solutions behave like Newtonian fluids at low shear frequency ($\omega < \omega_{crt}$). As ω increases above a critical frequency ω_{crt}, $\eta'(\omega)$ increases dramatically with increasing frequency and reaches a maximum $\eta'(\omega)$, i.e. η_{peak}', at ω_{peak}. As ω is higher than ω_{peak}, $\eta'(\omega)$ decreases dramatically with increasing ω. Similar $\eta'(\omega)$ behaviors of PDADMAC-1 and PDADMAC-2 aqueous solutions were also observed and those plots are not shown here. We define η_o' as the zero shear frequency viscosity of a solution, which can be obtained by extrapolating $\eta'(\omega)$ to $\omega = 0$; η_{peak}' the maximum $\eta'(\omega)$ of log $\eta'(\omega)$ versus log ω curve; ω_{crt} the frequency at which $\eta'(\omega)$ starts to increase as ω increases from a low to a high ω; ω_{peak} the shear frequency at which $\eta'(\omega_{peak}) = \eta_{peak}'$. In Fig. 5, the definitions of ω_{crt},

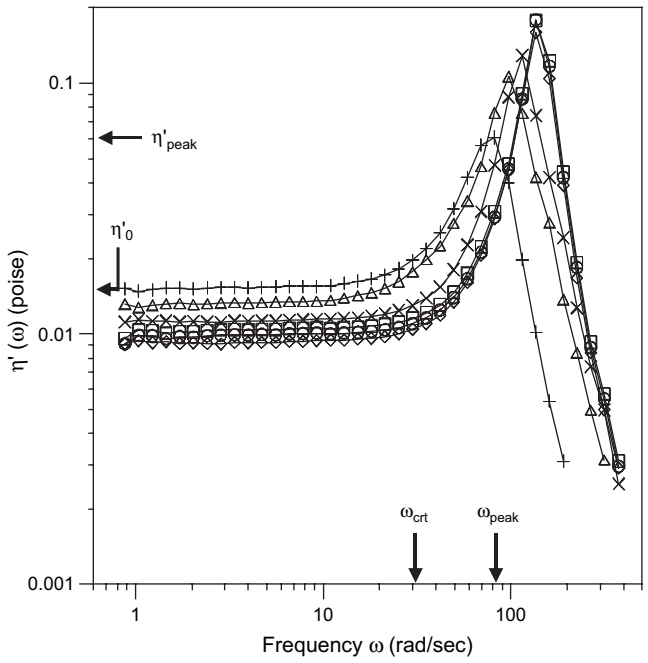

Fig. 5. Plots of DSV log $\eta'(\omega)$ versus log ω for 0.5 mg/ml PDADMAC-3 aqueous solutions mixed with various concentrations of NaCl. [NaCl]: (+) 0.0 M; (△) 0.04 M; (×) 0.07 M; (◇) 0.1 M; (□) 0.5 M; (○) 1.0 M. The designated arrows are ω_{crt}, ω_{peak}, η_o', and η_{peak}' of PDADMAC-3 aqueous solution mixed with 0.0 M NaCl.

ω_{peak}, η_o', and η_{peak}' for PDADMAC-3 aqueous solution mixed with 0.0 M NaCl are designated by arrows.

In literature [1,4,12–14,45], it has been reported that applying a shear force with increasing ω on polymer solutions causes formation and dissociation of inter-polymer aggregations. In Fig. 5, ω_{crt} ($\omega_{crt} = 10-30$ rad/s) is the lowest frequency for inducing polymer thickening and ω_{peak} ($\omega_{peak} = 70-200$ rad/s) the lowest frequency for breaking polymer aggregations. If ω_{crt} is lower than ω_{peak}, shear thickening behavior of polymer solutions will be observed. On the other hand, if the inter-polymers aggregation forces are weak and $\omega_{crt} > \omega_{peak}$, a shear thinning behavior will be observed. Shear field causes stretching of chains and increases the possibility for inter-polymer chain association, leading to an "upturn effect" of $\eta'(\omega)$ with increasing ω and thus a shear thickening behavior. It is obvious that ω_{peak} and η_{peak}' strongly depend on the polymer–polymer and polymer–solvent interactions. Increasing charge repulsion of polyions in solvents reduces the tendency for inter-polymer associations and leads to a reduction of the degree of shear thickening. Fig. 5 shows that both ω_{peak} and η_{peak}' increase with increasing NaCl concentration. These results suggest that mixing NaCl into PDADMAC aqueous solutions causes electrostatic shielding of $\geq N^+(CH_3)_2$ groups of PDADMACs by excess Cl^- ions and reduction of electrostatic charge repulsions of polyions, and thus enhancement of inter-polymer associations.

3.3.2. Storage and loss moduli

The rheometer with an oscillatory flow fluid in a tube permits examining not only viscosity $\eta'(\omega)$ but also elasticity $\eta''(\omega)$ of a solution. For a DVE measurement, viscosity η' is the ratio of shear stress component τ'', which is *in-phase* with shear rate $\acute{r}$, to the $\acute{r}$ (i.e. $\eta'(\omega) = \tau''(\omega)/\acute{r}(\omega)$). And, the elasticity η'' is the ratio of stress component τ', which is 90° *out-of-phase* with $\acute{r}$, to the $\acute{r}$ (i.e. $\eta''(\omega) = \tau'(\omega)/\acute{r}(\omega)$). $\eta''(\omega)$ relates to storage shear modulus $G'(\omega)$ by the equation $\eta''(\omega) = G'(\omega)/\omega$ and $\eta'(\omega)$ relates to the loss shear modulus $G''(\omega)$ by the equation $\eta'(\omega) = G''(\omega)/\omega$. During flow, η' can be attributed to the energy loss while η'' can be attributed to the energy storage through elastic deformation and inertia.

Since elasticity is an important DVE property of polymer solutions, in the following paragraphs we will show the ionic strength dependence of $G'(\omega)$ data and compare $G'(\omega)$ and $G''(\omega)$ data with Rouse and Zimm models' dilute polymer solutions. After that, we will analyze and compare $\eta'(\omega)$ data with DVE relaxation time $t_r(\omega)$ and shear rate at tube wall $\acute{r}_a(\omega)$. Based on the analyzed results, we propose a mechanism for the variation of polyion conformations with increasing ω (Section 3.3). Finally, we will discuss the ionic strength dependence of η_o' and η_{peak}' and thus the ionic strength dependence of shear thickening of polyions (Section 3.4).

Fig. 6 shows plots of log $G'(\omega)$ versus log ω for 0.5 mg/ml PDADMAC-3 aqueous solutions mixed with various concentrations of NaCl. The designated arrows shown in this figure are ω_{crt} and ω_{peak} of PDADMAC-3 aqueous solutions mixed with 1.0 M NaCl. These plots show two groups of $G'(\omega)$ data, i.e. one group of PDADMAC aqueous solutions mixed with [NaCl] ≤ 0.07 M and other group of PDADMAC aqueous solutions mixed with [NaCl] ≥ 0.1 M. At the shear frequency regime of 3 rad/s< ω < 70 rad/s, $G'(\omega)$ decreases with increasing NaCl concentration when [NaCl] ≤ 0.07 M, and $G'(\omega)$ does not vary significantly with NaCl concentration when [NaCl] ≥ 0.10 M. As will be shown in the discussions of Fig. 8 (a graph of $\eta'(\omega)$ with $t_r(\omega)$ and $\acute{r}_a(\omega)$), the oscillatory flow at the shear frequency regime of 3 rad/s < ω < 70 rad/s causes reduction of $t_r(\omega)$, which was attributed to intra-polymer associations. The presence of NaCl in PDADMAC aqueous solutions reduces electrostatic charge repulsions of polyions and enhances intra-polymer associations. Thus $G'(\omega)$ decreases with increasing NaCl concentration when ω is increased from 3 to 70 rad/s.

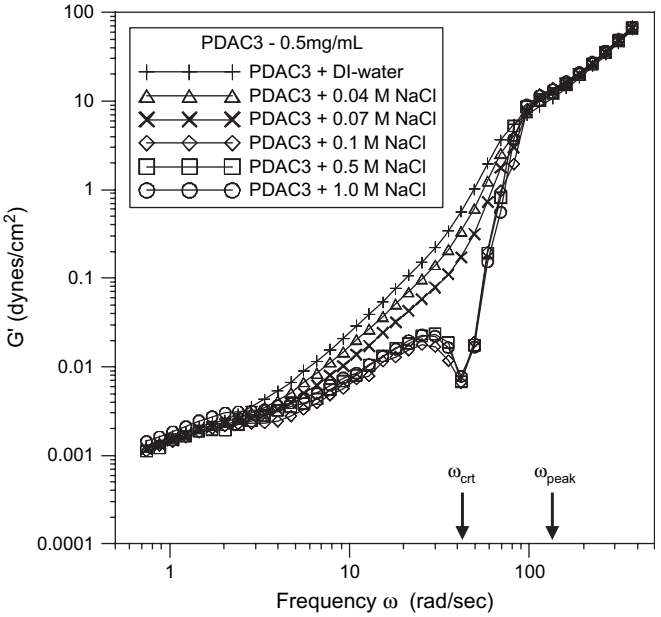

Fig. 6. Plots of log $G'(\omega)$ versus log ω for 0.5 mg/ml PDADMAC-3 aqueous solutions mixed with various concentrations of NaCl. [NaCl]: (+) 0.0 M; (△) 0.04 M; (×) 0.07 M; (◇) 0.1 M; (□) 0.5 M; (○) 1.0 M. The designated arrows are ω_{crt} and ω_{peak} of PDADMAC aqueous solution mixed with 1.0 M NaCl.

Fig. 6 shows that as ω < 1.5 rad/s, the log $G'(\omega)$ data of all the PDADAMAC-3 aqueous solutions are close but do not merge into one curve. The mixing of NaCl with PDADMAC aqueous solutions may cause a change of $G'(\omega)$ value, but the influence of NaCl concentration on $G'(\omega)$ in the frequency regime of ω < 1.5 rad/s is not so significant as in the frequency regime of 3 rad/s<ω < 70 rad/s. However, when ω is increased above 130 rad/s, all the log $G'(\omega)$ data merge into one curve with increasing ω. The frequency $\omega = 130$ rad/s is above the ω_{peak} of PDADMAC-3 aqueous solution mixed with 1.0 M NaCl, and thus is above the ω_{peak}s of all the PDADMAC-3 aqueous solutions (see Fig. 5: the solution with 1.0 M NaCl has a highest ω_{peak}). As will be shown in the top graphs of Fig. 8a and b, when $\omega > \omega_{peak}$, $\omega t_r/2\pi$ is larger than 1 (i.e. $t_r > 2\pi/\omega$, where t_r is the polymer relaxation time in unit of seconds). Thus the period $2\pi/\omega$ of the oscillatory flow is shorter than t_r, when $\omega > \omega_{peak}$. The relaxation of polymers

cannot keep pace with the alternating flow, most of energy are stored in the oscillatory flow. The $G'(\omega)$ relates to the viscoelastic property of local segments and increases with increasing ω and $G'(\omega)$ is independent of NaCl concentration.

$G''(\omega)$ is also an important viscoelastic property of polymer solutions. In literature, $G''(\omega)$ is combined with $G'(\omega)$ for the discussion of viscoelastic properties of polymer solutions. Fig. 7a and b shows plots of log $G''(\omega)$ and log $G'(\omega)$ versus log ω for 0.5 mg/ml PDADMAC-3 aqueous solutions mixed with 0.0 and 1.0 M NaCl, respectively. The plots of log $G''(\omega)$ and log $G'(\omega)$ versus log ω for 0.5 mg/ml PDADMAC-3 aqueous solutions mixed with 0.04 and 0.07 M NaCl are similar to those of PDADMAC-3 aqueous solution mixed with 0.0 M NaCl, and the plots of log $G''(\omega)$ and log $G'(\omega)$ versus log ω for 0.5 mg/ml PDADMAC-3 aqueous solutions mixed with 0.1 and 0.5 M NaCl are similar to those of PDADMAC-3 aqueous solution mixed with 1.0 M NaCl. Thus $G''(\omega)$ and $G'(\omega)$ plots of those solutions are not shown in the present paper.

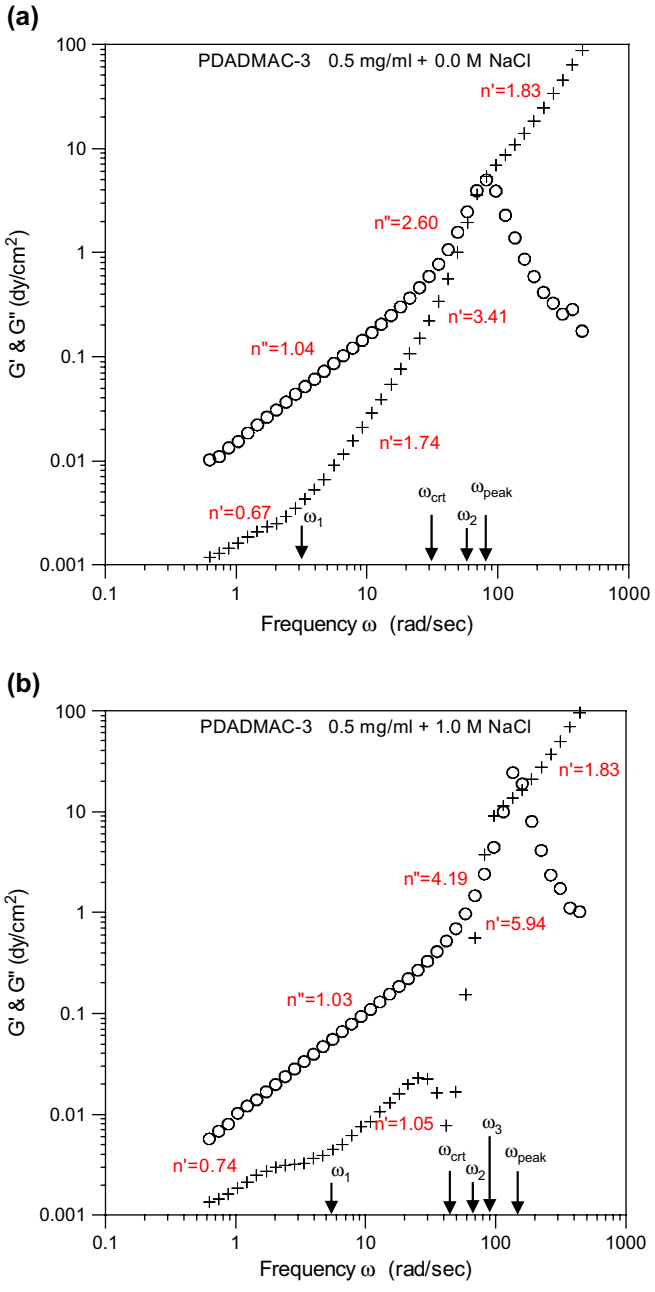

Fig. 7. Plots of log $G''(\omega)$ (○) and log $G'(\omega)$ (+) versus log ω for 0.5 mg/ml PDADMAC-3 aqueous solutions mixed with (a) (top) 0.0 M NaCl; (b) (bottom) 1.0 M NaCl. The numeric values are exponents n' of $G'(\omega)$ and n'' of $G''(\omega)$.

Comparing Fig. 7 with Fig. 5, we found the frequency ω at which $G' = G''$, i.e. $\tan\delta = 1$, is close to the ω_{peak} of $\eta'(\omega)$. As ω is above ω_{peak}, Fig. 7a and b shows that G' increases and G'' decreases with increasing ω, indicating polymer chains are highly elastic and less energy dissipates in the oscillatory flow. In ordinary dilute polymer solutions, the Rouse and Zimm models suggest $G'(\omega) \sim \omega^{n'}$ and $G'' \sim \omega^{n''}$ with $n' = 2$ and $n'' = 1$ when $\omega t_{r1}/2\pi < 1$ (where t_{r1} is the longest relaxation time of a polymer in solution), and log $G'(\omega)$ parallels to or merges with log $G''(\omega)$ with exponents $n' = n'' = 0.5$ and $n' = n'' = 0.67$ for Rouse and Zimm model solutions, respectively, when $\omega t_{r1}/2\pi > 1$ [46].

In Fig. 7a (with 0.0 M NaCl aqueous solution), the exponents n'' of $G''(\omega)$ are $n'' = 1.04$ when $\omega < \omega_{crt}$, $n'' = 2.60$ when $\omega_{crt} < \omega < \omega_{peak}$, and $n'' = -2.30$ when $\omega > \omega_{peak}$. The exponents n' of $G'(\omega)$ are $n' = 0.67$ when $\omega < \omega_1$, $n' = 1.74$ when $\omega_1 < \omega < \omega_{crt}$, $n' = 3.41$ when $\omega_{crt} < \omega < \omega_2$, and $n' = 1.83$ when $\omega > \omega_{peak}$. The exponent of $n'' = 1.04$ at the regime of $\omega < \omega_{crt}$ is consistent with the n'' exponent of ordinary dilute polymer solutions. However, the n' of $G'(\omega)$ for the whole frequency regime and n'' of $G''(\omega)$ for $\omega > \omega_{crt}$ indicate PDADMAC aqueous solutions have viscoelastic behaviors different from Rouse model and Zimm model polymer solutions.

In Fig. 7b (with 1.0 M NaCl aqueous solution), the n'' of $G''(\omega)$ are $n'' = 1.03$ when $\omega < \omega_{crt}$, $n'' = 4.19$ when $\omega_{crt} < \omega < \omega_{peak}$, and $n'' = -3.26$ when $\omega > \omega_{peak}$. The n' of $G'(\omega)$ are $n' = 0.74$ when $\omega < 20$ rad/s, $n' = 1.05$ when $\omega_1 < \omega < 30$ rad/s, $n' = 5.94$ when $\omega_{crt} < \omega < \omega_3$, and $n' = 1.83$ when $\omega > \omega_{peak}$. Similar to the PDADMAC aqueous solutions mixed with 0.0 M NaCl, the n' of G' for the whole frequency regime and n'' of G'' for $\omega > \omega_{crt}$ indicate 0.5 mg/ml PDADMAC aqueous solutions mixed with 1.0 M NaCl have viscoelastic behaviors different from Rouse and Zimm models' dilute polymer solutions. The reasons for the deviations of n' and n'' exponents of dilute PDADMAC aqueous solutions from those of Rouse and Zimm models' ordinary dilute polymer solutions will be discussed after the discussion of Fig. 8 (Section 3.4).

3.3.3. Comparison of DSV with relaxation time and shear rate

In a capillary rheometer, the shear rate $\acute{r}_o$ at tube wall of a Newtonian fluid is related to the volume flow rate U and tube radius a through the relation $\acute{r}_o = 4U/(\pi a^3)$. For a non-Newtonian fluid a Weissenberg–Rabinowitsch correction is needed, which is $\acute{r}_a = \acute{r}_o(3 + d\acute{r}_o/d\tau_a)/4$, where $\acute{r}_a$ is the shear rate and τ_a the shear stress at the tube wall [31,32,47]. The relaxation time t_r of a polymer in solution can be calculated from

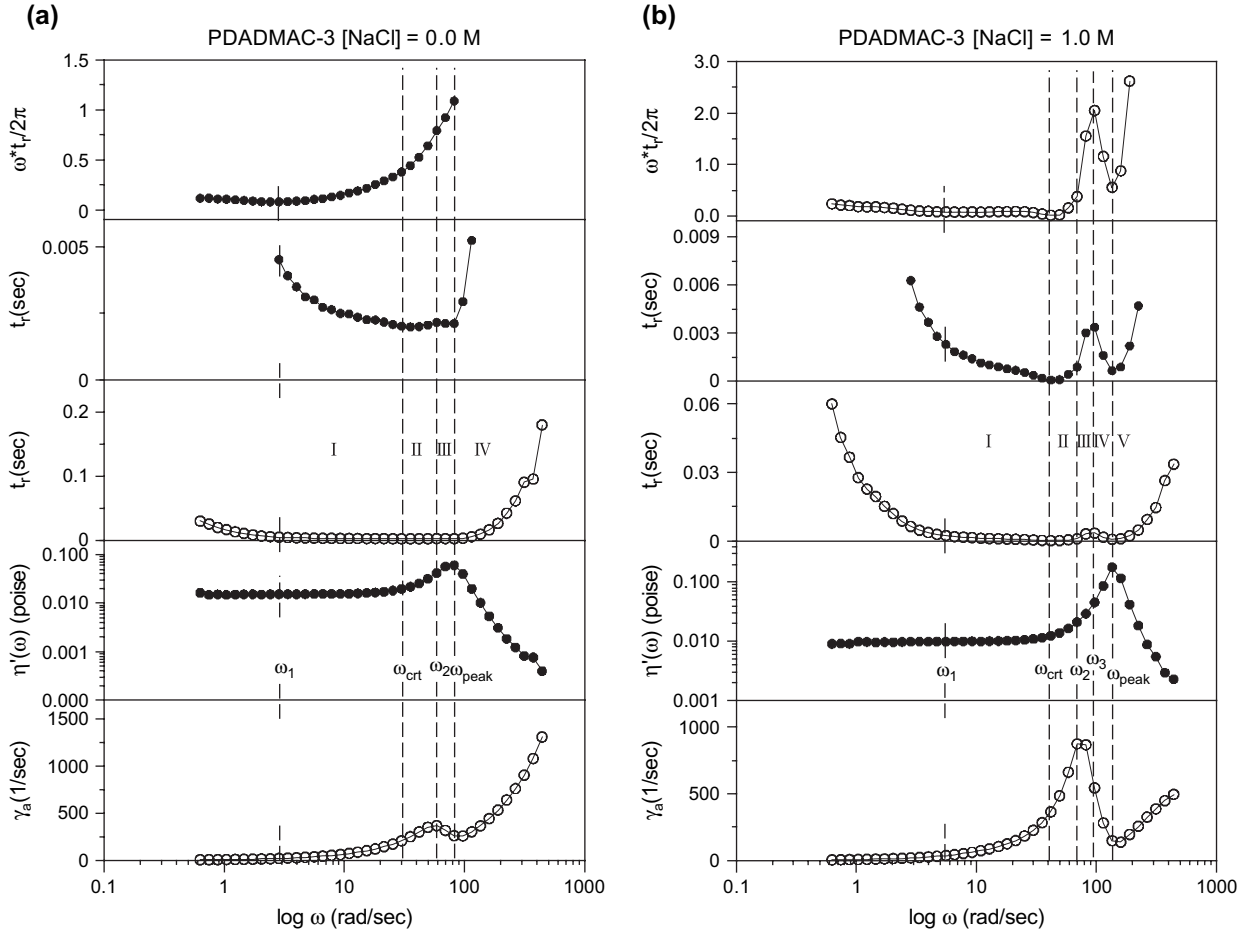

Fig. 8. Plots (from top to bottom) of $\omega t_r/2\pi$, t_r (with $\omega = 3.0-220$ rad/s), t_r (with $\omega = 0.6-400$ rad/s), $\eta'(\omega)$, and $\dot{\gamma}_a(\omega)$ versus log ω for 0.5 mg/ml PDADMAC-3 aqueous solution mixed with (a) 0.0 M NaCl; (b) 1.0 M NaCl.

viscoelasticity properties using the relation $t_r(\omega) = 2\pi G'(\omega)/\omega G''(\omega)$. The variation of $t_r(\omega)$ with ω gives information of the variation of polymer chain conformation with ω when $\omega t_r(\omega)/2\pi < 1$, i.e. $t_r < 2\pi/\omega$, the polymer relaxation time t_r is shorter than the period $2\pi/\omega$ of the oscillatory flow. In order to observe the variation of polymer chain conformation with increasing ω, we have plotted $\omega t_r(\omega)/2\pi$, $t_r(\omega)$, $\eta'(\omega)$, and $\dot{\gamma}_a(\omega)$ versus log ω in one graph for PDADMAC-3 aqueous solutions mixed with 0.0 M NaCl and 1.0 M NaCl and shown these plots in Fig. 8a and b, respectively. For the reason of easy viewing, the t_r axes (y-axes) of t_r versus log ω plots with $\omega = \sim 3.0-200$ rad/s were enlarged and are also shown in Fig. 8a and b. The graphs of the variations of PDADMAC molecular conformations with increasing ω in various frequency regimes are abstracted from Fig. 8a and b and shown in Fig. 9a and b, respectively.

In Figs. 8a and 9a (PDADMAC-3 aqueous solution mixed with 0.0 M NaCl), we divided the viscoelastic properties into several frequency regimes, i.e. regime-0 $\omega = 0$ rad/s, regime-I $\omega < \omega_{crt}$, regime-II $\omega_{crt} < \omega < \omega_2$, regime-III $\omega_2 < \omega < \omega_{peak}$, and regime-IV $\omega > \omega_{peak}$.

In regime-I ($\omega < \omega_{crt}$) of Fig. 8a, $\eta'(\omega)$ is independent of ω, indicating that the solution is in Newtonian flow region. The relaxation time $t_r(\omega)$ decreases when ω is increased from zero frequency to ω_1 and then decreased slowly as ω is increased from ω_1 to ω_{crt}. In regime-I, since the relaxation time of polymers is shorter than the period of an oscillatory flow (i.e. $\omega t_r(\omega)/2\pi < 1$), t_r can be related to the relaxation of a whole polymer chain. The oscillatory flow generated by the electrodynamic transducer induces intra-polymer contacts and thus intra-polymer associations (regime-0 and regime-I of Fig. 9a). The probability for intra-polymer associations increases with increasing ω when $\omega < \omega_{crt}$. The intra-polymer associations cause reduction of polymer particle sizes, thus $t_r(\omega)$ decreases and $\dot{\gamma}_a(\omega)$ increases with increasing ω when $\omega < \omega_{crt}$ (Fig. 8a). Two intra-polymer association processes may happen as ω is increased from $\omega = 0$ to $\omega = \omega_{crt}$. One is intra-polymer hydrophobic association and the other is intra-polymer ionic association of $\gtrdot N^+(CH_3)_2$ groups with Cl^- ions. For PDADMAC aqueous solutions without mixing with NaCl, the hydrophobic association is the major process of intra-polymer associations. Because of the positive electrostatic charge repulsions within a polymer chain, the intra-polymer ionic associations are not so significant as hydrophobic associations.

In regime-II ($\omega_{crt} < \omega < \omega_2$) of Fig. 8a, $\eta'(\omega)$ starts to increase, $t_r(\omega)$ increases slowly, and $\dot{\gamma}_a(\omega)$ continues increasing when ω is increased from ω_{crt} to ω_2. Dissociations of

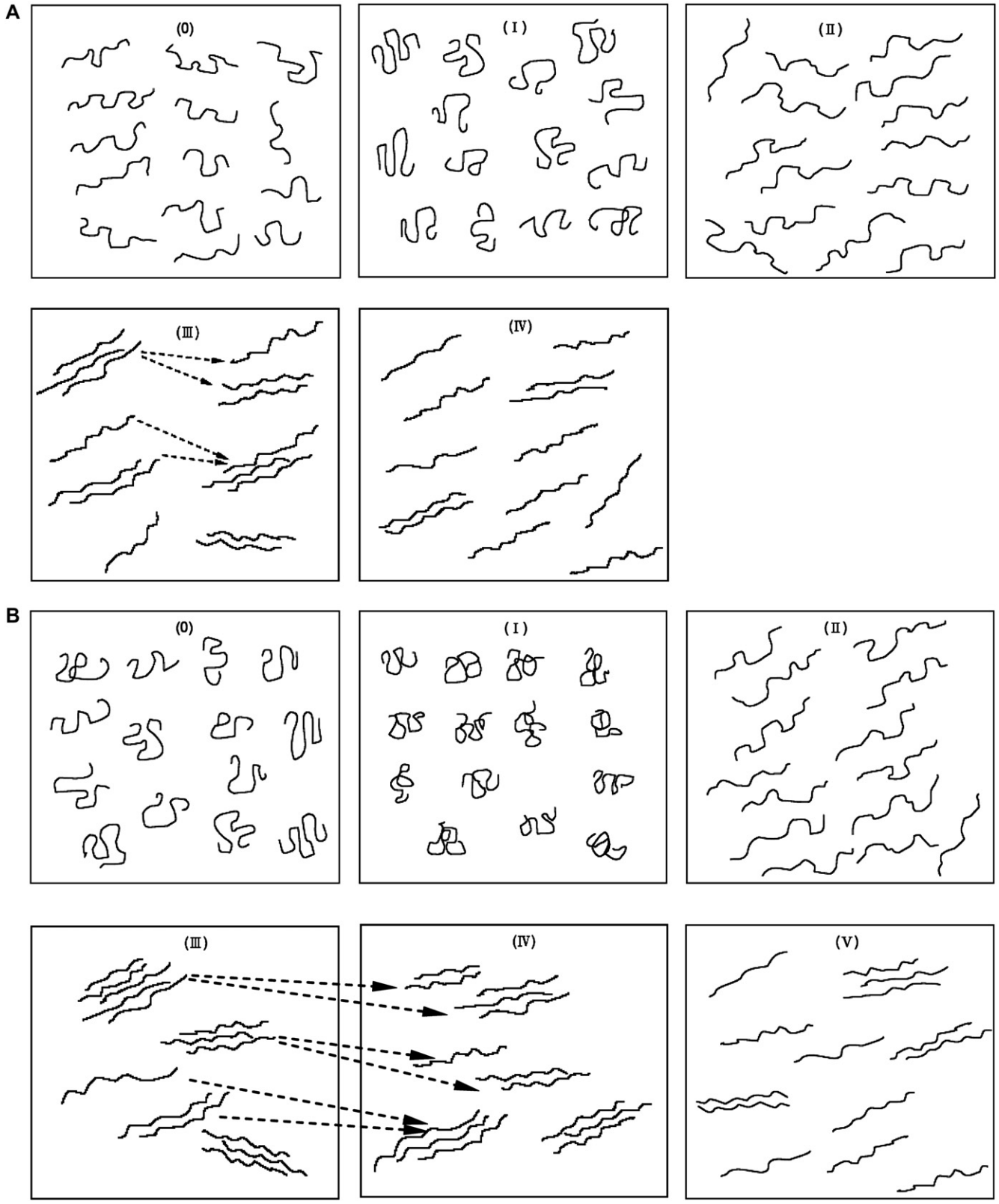

Fig. 9. Graphs of PDADMC conformations abstracted from Fig. 8 in various frequency regimes, for 0.5 mg/ml PDADMAC-3 aqueous solution mixed with (a) 0.0 M NaCl; (0) $\omega = 0$ rad/s; (I) $\omega < \omega_{crt}$; (II) $\omega_{crt} < \omega < \omega_2$; (III) $\omega_2 < \omega < \omega_{peak}$; (IV) $\omega_{peak} < \omega$. (b) 1.0 M NaCl. (0) $\omega = 0$ rad/s; (I) $\omega < \omega_{crt}$; (II) $\omega_{crt} < \omega < \omega_2$; $< \omega < \omega_2$; (III) $\omega_2 < \omega < \omega_3$; (IV) $\omega_3 < \omega < \omega_{peak}$; (V) $\omega_{peak} < \omega$.

intra-polymer associations and polymer chain expansions happen in this regime, thus $\eta'(\omega)$ and $t_r(\omega)$ increase with increasing ω (regime-II of Fig. 9a).

In regime-III ($\omega_2 < \omega < \omega_{peak}$) of Fig. 8a, $\eta'(\omega)$ increases and $\acute{r}_a(\omega)$ decreases when ω is increased from ω_2 to ω_{peak}. Inter-polymer aggregations happen in this regime, which causes increase of particle sizes and a further increase of $\eta'(\omega)$ and thus a decrease of $\acute{r}_a(\omega)$ with increasing ω. However, $t_r(\omega)$ does not vary significantly with ω when ω is increased from ω_2 to ω_{peak}, suggesting that dissociation of polymer chains from large inter-polymer aggregated particles may also occur simultaneously when ω is increased closer to ω_{peak} (regime-III of Fig. 9a).

In regime-IV ($\omega > \omega_{peak}$) of Fig. 8a, $\eta'(\omega)$ decreases, $\acute{r}_a(\omega)$ increases dramatically with increasing ω. The high frequency with short oscillation period causes polymer chains to have no time to form inter-polymer aggregations. Only dissociation of polymer chains from inter-polymer aggregations happen but no further inter-polymer aggregation proceeds in this regime. Particle sizes decrease and $\acute{r}_a(\omega)$ increases with increasing ω (regime-IV of Fig. 9a). However, the high stretching of polymer chains causes $t_r(\omega)$ to increase with increasing ω.

We also divide Figs. 8b and 9b (PDADMAC-3 aqueous solution mixed with 1.0 M NaCl) into several frequency regimes, i.e. regime-I $\omega < \omega_{crt}$, regime-II $\omega_{crt} < \omega < \omega_2$, regime-III $\omega_2 < \omega < \omega_3$, regime-IV $\omega_3 < \omega < \omega_{peak}$, and regime-V $\omega > \omega_{peak}$. Similar viscoelastic properties of Fig. 8b to those of Fig. 8a were observed with increasing ω in regime-I and regime-II, i.e. intra-polymer association in regime-I (regime-0 and regime-I of Fig. 9b), dissociation of intra-polymer association and chain expansion in regime-II (regime-II of Fig. 9b). Because of electrostatic charge repulsion caused by the shielding of $\rangle N^+(CH_3)_2$ groups of PDADMAC by excess Cl^- ions, the degree of intra-polymer associations are larger and the PDADMAC particle sizes are smaller in Fig. 8b than in Fig. 8a when $\omega < \omega_2$. Thus $t_r(\omega)$ is shorter and $\acute{r}_a(\omega)$ is larger in Fig. 8b than in Fig. 8a when $\omega < \omega_2$.

In regime-III ($\omega_2 < \omega < \omega_3$) of Fig. 8b, $\eta'(\omega)$ and $t_r(\omega)$ increase, and $\acute{r}_a(\omega)$ decreases with increasing ω, indicating inter-polymer aggregations happen in this regime, which causes increase of particle sizes and thus increase of $\eta'(\omega)$ and $t_r(\omega)$ and a decrease of $\acute{r}_a(\omega)$ (regime-III of Fig. 9b).

In regime-IV ($\omega_3 < \omega < \omega_{peak}$) of Fig. 8b, $\eta'(\omega)$ continues increasing, $\acute{r}_a(\omega)$ continues decreasing, and $t_r(\omega)$ decreases with increasing ω, suggesting inter-polymer aggregations of small polymer particles continue to proceed and dissociation of large inter-polymer aggregated particles happen simultaneously in this regime (regime-IV of Fig. 9b). Fig. 9b shows that some large aggregated particles dissociate into intermediate sizes particles and some small size particles aggregate into intermediate size particles as ω is increased from regime-III to regime-IV. The number of aggregated particles increases and the average particle sizes decrease as ω is increased from ω_3 to ω_{peak}. Thus $t_r(\omega)$ decreases (because of the decrease of average particle sizes) and $\acute{r}_a(\omega)$ also decreases (because of the increase of aggregated particle numbers) with increasing ω.

In regime-V ($\omega > \omega_{peak}$) of Fig. 8b, similar to that of Fig. 8a, $\eta'(\omega)$ decreases and $\acute{r}_a(\omega)$ increases dramatically with increasing ω. Only dissociations of polymer chains from inter-polymer aggregations proceed and no more inter-polymer aggregations happen in this regime, and the aggregated particle sizes decrease with increasing ω (regime-V of Fig. 9b).

After careful investigation of viscoelastic properties of Fig. 8a (0.5 mg/ml PDADMAC aqueous solution without mixing NaCl) and Fig. 8b (0.5 mg/ml PDADMAC aqueous solution mixed with 1.0 M NaCl), we found Fig. 8b had lower values of t_r and η' and higher value of $\acute{r}_a$ at $\omega = \omega_{crt}$ and $\omega = \omega_2$, and higher value of $\eta_{peak}{}'$ and lower value of $\acute{r}_a$ at $\omega = \omega_{peak}$ than Fig. 8a. The main reason for the difference in the viscoelastic properties of these two solutions is the difference in "*ionic strength*" of these two solutions. Mixing NaCl with PDADMAC aqueous solutions causes electrostatic shielding of $-N^+(CH_3)_2$ groups of PDADMAC and reduces electrostatic charge repulsion. The reduction of electrostatic charge repulsion results in the enhancement of intra-polymer association and thus the reduction of polymer particle sizes. Thus Fig. 8b shows lower t_r and η' and higher $\acute{r}_a$ at ω_{crt} and ω_2. Similarly, the presence of NaCl also reduces inter-polymer electrostatic charge repulsion, leading to the enhancement of inter-polymer aggregation. Thus Fig. 8b has higher $\eta_{peak}{}'$ and lower $\acute{r}_a$ than Fig. 8a at ω_{peak}.

3.3.4. The n' exponent of $G'(\omega)$ and relaxation time

Comparing n' exponents of Fig. 7a and b with t_r data of Fig. 8a and b, respectively, in the regimes of $\omega t_r/2\pi < 1$ (i.e. $\omega < \omega_{peak}$), we found $n' < 2$ when t_r decreases with increasing ω, and $n' > 2$ when t_r increases with increasing ω. Since the period of an oscillatory flow is longer than t_r when $\omega < \omega_{peak}$, t_r is related to the relaxation of a whole polymer chain when $\omega < \omega_{peak}$. The n' exponent with $n' < 2$ when ω is increased from zero frequency to ω_{crt}, can be attributed to the intra-polymer chain associations. The higher exponents of $n' > 2$ and $n'' > 1$ when ω is increased from ω_{crt} to ω_{peak} can be attributed to the polymer chain stretching and inter-polymer aggregations. The exponents of $n' = 1.83$ and $n'' < 0$ when $\omega > \omega_{peak}$ ($\omega t_r/2\pi > 1$) can be attributed to the dissociations of inter-polymer aggregations and high extension of polymer chains. The data of Fig. 7a and b also show that these two PDADMAC aqueous solutions have different n' exponents when $\omega < \omega_{crt}$. The smaller n' of Fig. 7b ([NaCl] = 1.0 M) than of Fig. 7a ([NaCl] = 0.0 M) when $\omega = 2.0$–40 rad/s indicates that the presence of NaCl reduces intra-polymer electrostatic charge repulsion and thus enhances intra-polymer association when ω is increased from 2.0 to 40 rad/s.

3.3.5. Degree of shear thickening and ionic strength

Fig. 10 shows the plots of $\eta_o{}'$ and $\eta_{peak}{}'$ versus NaCl concentration. These plots show that $\eta_o{}'$ increases with increasing PDADMAC molecular weight. $\eta_o{}'$ also decreases with increasing NaCl concentration, which is consistent with the NaCl concentration dependence of $\langle R_h \rangle$ data shown in Table 2 and can be attributed to the electrostatic shielding of $\rangle N^+(CH_3)_2$

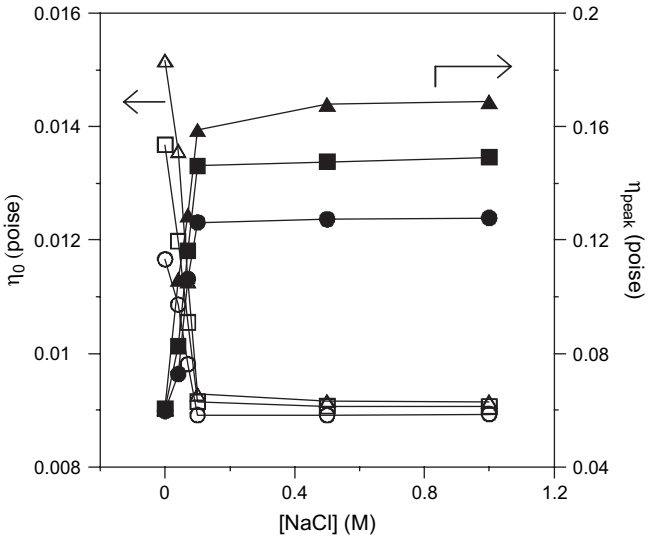

Fig. 10. Plots of η_o' and η_{peak}' of 0.5 mg/ml PDADMAC aqueous solutions versus NaCl concentration. η_{peak}': (●) PDADAMC-1; (■) PDADMAC-2; (▲) PDADMAC-3. η_o': (○) PDADAMC-1; (□) PDADMAC-2; (△) PDADMAC-3.

by the excess Cl^- ions. The electrostatic shielding of $\rangle N^+(CH_3)_2$ leads to the reduction of intra-polymer electrostatic charge repulsions and the shrinkage of polyion particles. These data also show that η_{peak}' increases with increasing NaCl concentration. Fig. 10 shows that η_{peak}' values of three different molecular weights of PDADMAC aqueous solutions mixed with 0.0 M NaCl were very close, in spite of different PDADMAC molecular lengths. As NaCl concentration was increased from 0.0 to 0.1 M the increment of η_{peak}' was larger for higher molecular weight PDADMAC, and the differences of η_{peak}' values among these three different molecular weights of PDADMAC solutions increased with increasing NaCl concentration. As NaCl concentration was higher than 0.1 M, the differences of η_{peak}' among these three different molecular weights of PDADMAC solutions did not change significantly with increasing NaCl concentration.

As discussed in previous sections, applying a shear field on a polyion solution results in the stretching of polymer chains and the aggregation of stretched polyions. Thus shear thickening occurs when a polyion solution is under a shear field. The η_{peak}' data of solutions with [NaCl] = 0.0 M shown in Fig. 10 suggest the sizes of aggregated charged particles increased with increasing ω while $\omega_{crt} < \omega < \omega_{peak}$ and the aggregated charged particle sizes would not increase any more when the sizes of the particles reached a "*critical size*", because of high charges of particles. When the charge of aggregated particles reaches a critical charge number, no further association of polyion chains into the aggregated particles happens, because of high electrostatic charge repulsion from the aggregated particles. The sizes of an aggregated charged particle depend on the total charges of the aggregated particle, but not on the polyion chain lengths inside the charged aggregated particles. Fig. 11a shows that at $\omega = \omega_{peak}$ for two different molecular weights of PDADMAC aqueous solutions without mixing NaCl, the sizes and total charges of these two aggregated PDADMAC particles are the same, in spite of different polyion chain lengths within the aggregated particles. The electrostatic charge repulsions of these two aggregated particles are same. Thus η_{peak}' was independent of PDADMAC molecular weight when [NaCl] = 0.0 M in the aqueous solutions. When NaCl was mixed with PDADMAC aqueous solutions, because the charges of polyions are shielded by excess Cl^-, in a shear field the stretched polymer chains of longer chain lengths have more chance to contact with other polymer

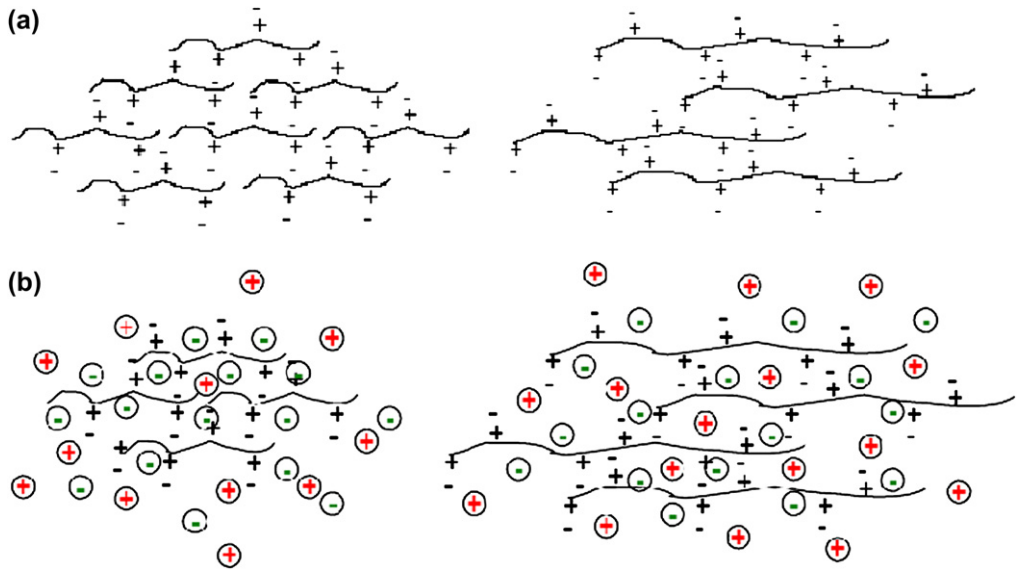

Fig. 11. (a) The PDADMAC polymer chains at a shear frequency $\omega = \omega_{peak}$ in aqueous solutions without mixing NaCl: (left figure) low M_w PDADMAC solution; (right figure) high M_w PDADMAC solution. (b) The PDADMAC polymer chains at a shear frequency $\omega = \omega_{peak}$ in aqueous solutions mixed with NaCl. ⊕: Na^+; ⊙: Cl^-; (+) positive charge of PDADMAC; (−) negative charge of counter ions. (left figure) low M_w PDADMAC solution; (right figure) high M_w PDADMAC solution.

chains and form larger aggregated particles than those of shorter chain lengths (Fig. 11b). Thus Fig. 10 shows that the solutions of higher molecular weight PDADMAC had higher η_{peak}' values than those solutions of lower molecular weight PDADMAC when NaCl concentration is above 0.04 M.

In Table 3, we summarize η_{peak}'/η_o' ratios of PDADMAC aqueous solutions. These results show that when [NaCl] $\geq$ 0.04 M and at a fixed NaCl concentration η_{peak}'/η_o' increased with increasing PDADMAC molecular weight, suggesting that the degree of shear thickening increased with increasing PDADMAC molecular weight when [NaCl] $\geq$ 0.04 M. Table 3 also shows that at a fixed PDADMAC molecular weight, η_{peak}'/η_o' increases with increasing NaCl concentration, suggesting the enhancement of shear thickening by the presence of NaCl in the solutions. The increment of the degree of shear thickening was due to the electrostatic shielding of $-N^+(CH_3)_2$ groups of PDADMACs by excess Cl^- ions and a reduction of inter-polymer charge repulsions by the presence of excess salt NaCl.

3.4. Comparison of dynamic shear viscosity with DLS hydrodynamic radius

In Fig. 12, we plot log η_o' versus log $\langle R_h \rangle$ for PDADMAC aqueous solutions mixed with various concentrations of NaCl. Two groups of data were observed in Fig. 12, i.e the data with high zero shear viscosities log $\eta_o' = -2.03$ to -1.82 poise ([NaCl] $\leq$ 0.07 M) and the data with low shear viscosities log $\eta_o' = -2.06$ to -2.03 poise ([NaCl] $\geq$ 0.10 M). The slopes 0.474 and 0.0497 of log η_o' against log $\langle R_h \rangle$ were obtained for high viscosity solutions ([NaCl] $\leq$ 0.07 M) and low viscosity solutions ([NaCl] $\geq$ 0.10 M), respectively. It is known that mixing excess salt into polyion solutions results in the shielding of electrostatic charges on polyions and thus the reduction of surface charges of polyions. These results are similar to the results shown in Fig. 10. Fig. 10 shows no significant difference in η_o' data of PDADMAC aqueous solutions when NaCl concentration was above 0.10 M. However, as NaCl concentration was lower than 0.07 M, η_o' increased dramatically as NaCl concentration was decreased. The different particle sizes $\langle R_h \rangle$ dependencies of η_o' between PDADMAC aqueous solutions containing [NaCl] $\leq$ 0.07 M and those containing [NaCl] $\geq$ 0.10 M can be attributed to the different polyion chains conformations, i.e. rod-like PDADMAC structures for [NaCl] $\leq$ 0.07 M and coiled-like structures for [NaCl] $\geq$ 0.10 M, resulted from different polyion charge densities due to different ionic strengths in the solutions.

Table 3
Ratio of η_{peak}'/η_o' of 0.5 mg/ml PDADMAC aqueous solutions mixed with various concentrations of NaCl

	[NaCl]					
	0.0 M	0.04 M	0.07 M	0.1 M	0.5 M	1.0 M
PDADMAC-1	5.12	6.69	10.83	14.16	14.29	14.31
PDADMAC-2	4.41	6.90	11.02	15.98	16.27	16.47
PDADMAC-3	3.99	7.82	11.42	17.12	18.32	18.45

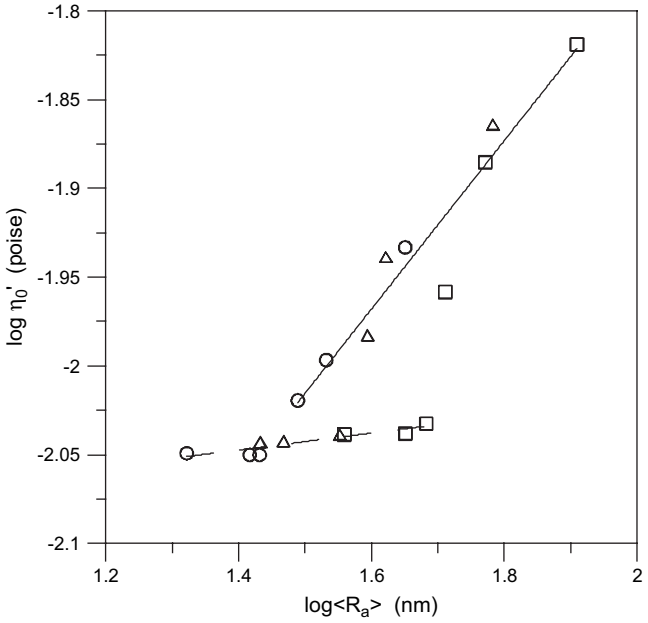

Fig. 12. Plot of log η_o' versus log $\langle R_h \rangle$ for three PDADMAC aqueous solutions. (○) PDADAMC-1; (△) PDADMAC-2; (□) PDADMAC-3. The slopes of log η_o versus log $\langle R_h \rangle$ are 0.0497 and 0.474 for low η_o' ([NaCl] $\geq$ 0.10 M, dashed fitted line) and high η_o' ([NaCl] $\leq$ 0.07 M, solid fitted line), respectively.

In the following paragraphs, by comparing DLS $\langle R_h \rangle$ data with DSV η' data, we show that inter-polymer aggregations may happen in a dilute solution (the polymer concentration is lower than the overlap concentration C^*) when it is under an oscillatory flow.

In dilute PDADMAC aqueous solutions ([PDADMAC] = 0.5 mg/ml in the present study), polymer chains are well separated from each other and few inter-polymer chain aggregations occurs. Since the compatibility of water with PDADMAC backbones is poor, increasing ionic strength (i.e. increasing NaCl concentration) of dilute PDADMAC aqueous solutions causes intra-molecular association and leads to shrinkages of polymer chains and $\langle R_h \rangle$ decreases with increasing NaCl concentration as shown in Table 2. However, inter-polymer chain aggregations may happen in dilute solutions when polymer chains are fully stretched. For example, the fully extended PDADMAC-1 had a contour length of 343.9 nm (Table 4). The overlap concentration C^*_{str} of a fully stretched PDADMAC-1 aqueous solution is

$$C^*_{str} = M_w / \left[(4/3)\pi N_A (L_c/2)^3\right] = 151{,}000 \times 10^3 \text{ mg} / \left[(4/3)\pi \left(6.03 \times 10^{23}\right) \times \left(343.9 \times 10^{-7} \text{ cm}/2\right)^3\right] = 1.18 \times 10^{-2} \text{ mg/ml} \quad (4)$$

The PDADMAC concentration, i.e. 0.5 mg/ml, in the present study was much higher than $C_{str}^* = 1.18 \times 10^{-2}$ mg/ml, and thus inter-polymers chain associations might happen when PDADMAC molecular chains were fully stretched.

Table 4
PDADMAC counter length L_c, $L_c/2R_G$ and $[\eta_{peak}/\eta_o]'$

Solution	L_c (nm)	$L_c/2R_G$[a]	$[\eta_{peak}/\eta_o]' = [L_c/2R_G]^{0.474}$
0.0 M NaCl			
PDADMAC-1	343.9	1.92	1.36
PDADMAC-2	535.2	2.17	1.44
PDADMAC-3	1015.7	3.13	1.72
0.04 M NaCl			
PDADMAC-1	343.9	2.66	1.59
PDADMAC-2	535.3	3.36	1.78
PDADMAC-3	1015.7	4.53	2.05
0.07 M NaCl			
PDADMAC-1	343.9	3.10	1.71
PDADMAC-2	535.3	3.78	1.88
PDADMAC-3	1015.7	5.49	2.24
0.1 M NaCl			
PDADMAC-1	343.9	3.83	1.89
PDADMAC-2	535.3	4.20	1.97
PDADMAC-3	1015.7	6.00	2.34
0.5 M NaCl			
PDADMAC-1	343.9	3.90	1.91
PDADMAC-2	535.3	5.45	2.23
PDADMAC-3	1015.7	6.80	2.48
1.0 M NaCl			
PDADMAC-1	343.9	4.83	2.11
PDADMAC-2	535.3	5.89	2.32
PDADMAC-3	1015.7	8.25	2.72

[a] R_G calculated from R_h by assuming: $R_G = 1.7R_h$ for [NaCl] $\geq$ 0.1 M; $R_G = 1.8R_h$ for [NaCl] = 0.07 M; $R_G = 1.9R_h$ for [NaCl] = 0.04 M; $R_G = 2.0R_h$ for [NaCl] = 0.0 M.

The three PDADMAC contour lengths L_c were calculated using Eq. (5) and are summarized in Table 4.

$$L_c = l_o(M_n/M_o) \tag{5}$$

where $M_o = 161.5$ g/mol is the mass of a monomer unit and $l_o = 0.55$ nm the length of a unit monomer [27]. We assumed a polydispersity of $M_w/M_n = 1.5$, and calculated M_n from M_w, which were obtained from SLS measurements of PDADMAC aqueous solutions mixed with 1.0 M NaCl (Table 1). These M_n data were used in Eq. (5) for L_c calculations. Though this calculation is rough, these data are still good for qualitative analyses.

As mentioned in Section 2, the ratio $\langle R_G\rangle/\langle R_h\rangle$ is an indicator of the compactness of polymers in solvents. According to Burchard [44], $\langle R_G\rangle/\langle R_h\rangle > 2.0$ for rod structural polymers and $\langle R_G\rangle/\langle R_h\rangle = 1.78-1.50$ for polydispersed random coiled polymers. In Section 2, we have shown $\langle R_G\rangle/\langle R_h\rangle$ ratios of around 1.68–1.69 for 0.5 mg/ml PDADMAC in 1.0 M NaCl aqueous solution. From η_o' data shown in Fig. 10, it is reasonable to assume $\langle R_G\rangle/\langle R_h\rangle = 1.70$, i.e. coiled-like structures, for PDADMAC aqueous solutions with [NaCl] $\geq$ 0.1 M, and $\langle R_G\rangle/\langle R_h\rangle = 2.0$, i.e. rod-like structures, for PDADMAC aqueous with [NaCl] = 0.0 M. The η_o' (Fig. 10) values of PDADMAC aqueous solutions with [NaCl] = 0.04 and 0.07 M located between those of PDADMAC aqueous solutions with [NaCl] = 0.1 and 0.0 M, indicate that PDADMAC molecular chains have conformations behaving in the intermediate range between rod-like and coil-like structures. Thus we assumed $\langle R_G\rangle/\langle R_h\rangle = 1.9$ and 1.8 for PDADMAC aqueous solutions mixed with NaCl concentrations of 0.04 and 0.07 M, respectively. Using these assumptions, we obtained $\langle R_G\rangle$ values from $\langle R_h\rangle$ (Table 2) and calculated $L_c/2R_G$ data. The values of $L_c/2R_G$, an indicator of chain stretching ratio, are summarized in Table 4. Comparing $L_c/2R_G$ ratios listed in Table 4 with η_{peak}'/η_o' ratios listed in Table 3, we found that $L_c/2R_G$ ratios were smaller than η_{peak}'/η_o' ratios. Using the relation $[\eta_{peak}/\eta_o]' = [L_c/2R_G]^{0.474}$ (the exponent "0.474" is obtained from the plot of log η_o' against log $\langle R_h\rangle$ for PDADMAC aqueous solutions with [NaCl] $\leq$ 0.07 M shown in Fig. 12), we calculated $[\eta_{peak}/\eta_o]'$ from $[L_c/2R_G]$ and the calculated $[\eta_{peak}/\eta_o]'$ data are shown in Table 4. Comparing the calculated $[\eta_{peak}/\eta_o]'$ data with the experimental η_{peak}'/η_o' data (Table 3), we found the calculated $[\eta_{peak}/\eta_o]'$s were smaller than the measured η_{peak}'/η_o' ratios. These results suggest that shear thickening in dilute PDADMAC aqueous solutions comes not only from polymer chain stretching but also from inter-polymer chain aggregations.

4. Conclusions

Using DLS and DVE measurements, the dilute solution properties of three different MW PDADMAC aqueous solutions mixed with various concentrations of NaCl were investigated. In the DVE measurements with increasing ω, we showed that the lower n' exponent of $G'(\omega)$ with $n' < 2$ and a constant $\eta'(\omega)$ value when $\omega < \omega_{crt}$; and the higher n' exponent with $n' > 2$ and the upturn of $\eta'(\omega)$ when $\omega_{crt} < \omega < \omega_{peak}$. By analyzing $\eta'(\omega)$, $t_r(\omega)$, and $\acute{r}_a(\omega)$ of PDADMAC aqueous solutions in oscillatory flows, we proposed changes of polymer chain conformations with increasing ω via the following steps: intra-polymer associations ($\omega < \omega_{crt}$), dissociation of intra-polymer associations ($\omega_{crt} < \omega < \omega_2$), stretching of polymer chains ($\omega_2 < \omega < \omega_3$), inter-polymer aggregations ($\omega_3 < \omega < \omega_{peak}$), and dissociations of inter-polymer aggregations ($\omega_{peak} < \omega$). The lowering of n' with $n' < 2$ was attributed to the intra-polymer association and the upturn of $\eta'(\omega)$ was attributed to the stretching of polymer chains and inter-polymer aggregations. By comparing DSV η' data with DLS hydrodynamic radii (R_h) data, we confirmed the possibility of inter-polymer aggregations in the dilute solutions, which leads to the shear thickening of the solutions. Two major polymer association processes may happen during the oscillating flow. One is the hydrophobic association and the other is the ionic association of $-N^+(CH_3)_2$ groups of PDADMC via counter ions and excess Cl^- ions. The intra-polymer associations ($\omega < \omega_{crt}$) and shear thickening ($\omega_3 < \omega < \omega_{peak}$) behaviors were favored by increasing ionic strength of solutions. Mixing NaCl into dilute PDADMAC aqueous solutions resulted in electrostatic shielding of ionic $-N^+(CH_3)_2$ groups of PDADMC by excess Cl^- ions, and a lowering of electrostatic charge repulsions among the PMADMAC molecules. Thus intra-polymer associations and shear thickening resulted from the inter-polymer chain

aggregations were enhanced by increasing NaCl concentration in the solutions.

References

[1] Kishbaugh AJ, MaHugh AJ. Rheol Acta 1993;32(9–24):115–31.
[2] Layec-Raphalen MN, Welff C. J Non-Newtonian Fluid Mech 1976;1: 159–73.
[3] Georgelos PN, Torkelson JM. Rheol Acta 1988;27:369–83.
[4] Vrahopoulou EP, McHugh A. J Non-Newtonian Fluid Mech 1987;25: 157–75.
[5] Georgelos PN, Torkelson JM. J Non-Newtonian Fluid Mech 1988;27: 191–204.
[6] Biggs S, Selb J, Candau F. Polymer 1993;34:580–91.
[7] Yu TL, Lu WC, Liu WH, Lin HL, Chiu CC. Polymer 2004;45:5579–89.
[8] Chang Y, McCormick CL. Polymer 1994;35:3503–12.
[9] Cabane B, Wong K, Linder P, Laufma F. J Rheol 1997;41:531–47.
[10] Bokias G, Hourdet D, Illiopoulos I. Macromolecules 2000;33:2929–35.
[11] Inoue T, Osaki K. Rheol Acta 1993;32:550–5.
[12] Wolff C. Adv Colloid Interface Sci 1982;17:263–74.
[13] Dupuis D, Wolff C. Chem Eng Commun 1985;32:203–17.
[14] Vrahopoulou EP, McHugh AJ. Chem Eng Commun 1987;57:289–95.
[15] Witten TA, Cohen MH. Macromolecules 1985;18:1915–8.
[16] Ballard MJ, Buscall R, Watte FA. Polymer 1988;29:1287–93.
[17] Barnes HA. J Rheol 1989;33:329–66.
[18] Marrucci G, Bhargava S, Cooper SL. Macromolecules 1993;26:6483–8.
[19] Wang SQ. Macromolecules 1992;25:7003–10.
[20] Ma SX, Cooper SL. Macromolecules 2001;34:3294–301.
[21] Hatzikiriakos SG, Vlassopoulos D. Rheol Acta 1996;35:274–87.
[22] Edwards BJ, Keffer DJ, Reneau CW. J Appl Polym Sci 2002;85: 1714–35.
[23] Jiang B, Keffer DJ, Edwards BJ, Alfred JN. J Appl Polym Sci 2003;90: 2997–3011.
[24] Lancaster JE, Baccei L, Panzer HP. J Polym Sci Polym Lett Ed 1976;14: 549–54.
[25] Kabanov VA, Topchiyev DA. Polym Sci USSR 1988;30:667–71.
[26] Jaeger W, Hanhn M, Lieske A, Zimmermann A, Brand F. Macromol Symp 1996;111:95–106.
[27] Dautzenberg H, Gornitz E, Jaeger W. Macromol Chem Phys 1998;199: 1561–71.
[28] Ali SKA, Ali A. Polymer 2001;42:7961–70.
[29] Burkhardt CW, McCarthy KJ, Parazak DP. J Polym Sci C Polym Lett 1987;25:209–13.
[30] Koslov GV, Malkanduev YA, Zaikov GE. J Appl Polym Sci 2004;91: 3144–7.
[31] Thurston GB. J Acoust Soc Am 1960;32:210–3.
[32] Thurston GB. Biorheology 1976;13:191–9.
[33] Vilastic Sci. Inc.. Operational manual, vilastic viscoelasticity analyzer. Austin: Vilastic Scientific Inc.; 2000.
[34] C.N. Wood Mfg. Co.. Operation manual for differential refractometer model RF-600. Newton, PA: C.N. Wood Mfg. Co.; 1991.
[35] Brookhaven Inc. Corp.. Instruction manual for model BI-2030AT digital correlator. New York: Brookhaven Instruments Inc. Corp.; 1986.
[36] Evans JM. In: Huglin MB, editor. Light scattering from polymer solutions. London: Academic Press; 1972 [chapter 5].
[37] Sedlak M. In: Brown W, editor. Light scattering – principles and development. Oxford: Clarendon Press; 1996 [chapter 4].
[38] Sedlak M, Amis EJ. J Chem Phys 1992;96:817–25.
[39] Xia J, Dubin PL, Izumi T, Hirata M, Kokufuta E. J Polym Sci B Polym Phys 1996;34:497–503.
[40] Lin SC, Lee WI, Shurr JM. Biopolymers 1978;17:1041–64.
[41] Sedlak M, Konak C, Stepanek P, Jakes J. Polymer 1987;28:873–80.
[42] Forster S, Schmidt M, Antonietti M. Polymer 1990;31:781–91.
[43] Sedlak M. Langmuir 1999;15:4045–51.
[44] Burchard W. In: Brown W, editor. Light scattering – principles and development. Oxford: Clarendon Press; 1996 [chapter 13].
[45] Peiffer DG, Lundberg RD, Duvdevani I. Polymer 1986;27:1453–62.
[46] Ferry JD. Viscoelastic properties of polymers. 3rd ed. John Wiley & Sons, Inc; 1980 [chapter 9].
[47] Morrison FA. Understanding rheology. New York: Oxford University Press; 2001. p. 391, [chapter 10].